ATLAS NOTE

ATLAS-CONF-2014-014

March 25, 2014

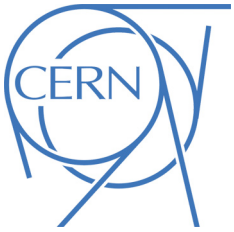

Search for the direct pair production of top squarks decaying to a b-quark, a tau lepton, and weakly interacting particles in $\sqrt{s} = 8$ TeV pp collisions using 20 fb^{-1} of ATLAS data

The ATLAS Collaboration

Abstract

Preliminary results of a search for direct pair production of supersymmetric partners of the top quark decaying via a τ slepton and with a gravitino in the final state ($\tilde{t}_1 \to b\nu_\tau\tilde{\tau}_1 \to b\nu_\tau\tau\tilde{G}$) are reported. Top squarks are searched for in events with two leptons (electrons or muons) in the final state using 20.3 fb^{-1} of integrated luminosity from LHC pp collisions at $\sqrt{s} = 8$ TeV collected by the ATLAS detector. No excess above the Standard Model expectation is observed. Exclusion limits at 95% confidence level are placed as a function of the top squark and τ slepton masses. Models where the mass difference between the top squark and the τ slepton is below 35 GeV are excluded at 95% CL for top squark masses up to 480 GeV. Top squark masses below 170 GeV are excluded for all τ slepton mass values.

1 Introduction

Partners of the top quark are an ingredient of several models addressing the hierarchy problem [1–4] of the Standard Model (SM). A boson partner would stabilize the Higgs boson mass against quadratically divergent quantum corrections, provided its mass is close to the electroweak symmetry breaking energy scale, making it accessible at the LHC [5]. One of these models is supersymmetry (SUSY) [6–14] which naturally resolves the hierarchy problem by introducing supersymmetric partners of the known bosons and fermions. In a generic R-parity conserving minimal supersymmetric extension of the SM (MSSM) [15–19] the scalar partners of right-handed and left-handed quarks, $\tilde{q}_R$ and $\tilde{q}_L$, and charged leptons, $\tilde{l}_R$ and $\tilde{l}_L$, can mix to form two squark and two slepton mass eigenstates. The lighter of the two top squark eigenstates is denoted as $\tilde{t}_1$ and is referred to as the top squark in the following. Likewise, the lighter of the two τ slepton eigenstates is denoted $\tilde{\tau}_1$ and referred to as the τ slepton in the following.

In gauge-mediated supersymmetry breaking (GMSB) models the spin 3/2 partner of the graviton, called the gravitino, is expected to be the lightest supersymmetric particle. Assuming that the mass scale of the messengers responsible for the supersymmetry breaking is of the order of 10 TeV, in order to have low fine tuning [20], the top squark is expected to be lighter than about 400 GeV [21]. If the τ slepton is lighter and the supersymmetric partners of the gauge and Higgs boson are heavier than the top squark, the dominant decay mode of the $\tilde{t}_1$ can be the three-body decay into $b\nu_\tau\tilde{\tau}_1$, followed by the $\tilde{\tau}_1$ decay into a τ lepton and the gravitino. This is illustrated in Figure 1. No limits have been published so far from hadron collider searches for this decay mode, whilst the LEP experiments place a lower limit of 87 GeV on the mass of the τ slepton [22–26].

Previous searches for top squark pair production performed by the ATLAS collaboration in the fully hadronic final states [27,28] and in final states with one electron or muon [29] are expected to have limited sensitivity to the decay mode with two τ leptons in the final state, because they have dedicated selections to reduce the background from pair production of top quarks with at least one of them decaying via a hadronic τ. The search with two electrons or muons, referred to also as ℓ in the following, in the final state [30] is expected to have sensitivity to events where both τ leptons decay leptonically. Exclusion limits obtained by reinterpreting the results of Ref. [30] are reported, as well as a new search specifically targeting small $\tilde{t}_1$ and $\tilde{\tau}_1$ masses.

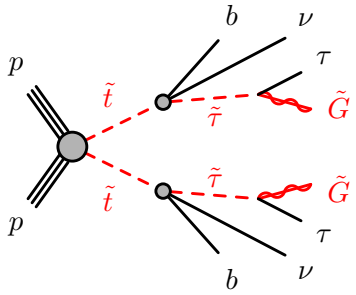

Figure 1: The diagram illustrates the production of a top squark pair, where each top squark undergoes a three-body decay into $b\nu_\tau\tilde{\tau}_1$, followed by the $\tilde{\tau}_1$ decay into a τ lepton and the gravitino.

2 The ATLAS detector

The ATLAS detector [31] consists of inner tracking devices surrounded by a superconducting solenoid, electromagnetic and hadronic calorimeters and a muon spectrometer with a toroidal magnetic field. The

Table 1: The Monte Carlo samples used to simulate the most important SM background processes with prompt leptons in the final state. The ALPGEN and MC@NLO samples have been interfaced to HERWIG-6.5.20 [32] for the fragmentation and hadronization description, while MADGRAPH samples have been interfaced with PYTHIA-6.426 [33] for the same purpose.

Physics process	generator	Reference
$Z/\gamma^\star \to \ell\ell, m(\ell\ell) > 40$ GeV	SHERPA 1.4.1	[34]
Drell-Yan, $m(\ell\ell) < 40$ GeV	ALPGEN 2.14	[35]
$t\bar{t} \to \ell + X$ and Wt	MC@NLO-4.06	[36, 37]
$t\bar{t}W$ and $t\bar{t}Z$	MADGRAPH-5.1.4.8	[38]
WW,WZ,ZZ	POWHEG 1.0	[39]

inner detector, in combination with the axial 2 T field from the solenoid, provides precision tracking of charged particles for $|\eta| < 2.5$ [1]. It consists of a silicon pixel detector, a silicon strip detector and a straw tube tracker that also provides transition radiation measurements for electron identification. The calorimeter system covers the pseudorapidity range $|\eta| < 4.9$. It is composed of sampling calorimeters with either liquid argon or scintillating tiles as the active media. The muon spectrometer has separate trigger and high-precision tracking chambers which provide muon trigger and measurement capabilities for $|\eta| < 2.4$ and $|\eta| < 2.7$, respectively.

3 Data and Monte Carlo samples

The search reported in Ref. [30] and the new selection reported here share the same dataset and trigger strategy. Proton-proton collisions at a centre-of-mass energy of 8 TeV are used. Events are required to pass either a single-electron, a single-muon, a double-electron, a double-muon, or an electron-muon trigger. The trigger efficiency exceeds 99% for the events passing the full selection described in Section 5. After beam, detector and data quality requirements, a total integrated luminosity of $(20.3 \pm 0.6)\,\text{fb}^{-1}$ is used.

Several Monte Carlo (MC) simulated event samples are used to estimate the signal yields and to aid in the description of the SM background processes leading to two prompt leptons. For the larger SM contributions, the shape of distributions of kinematic variables is taken from simulation, while the normalization is determined by measurements in appropriate data control regions as described in Ref. [30]. For the smaller backgrounds with two prompt leptons and for the signal, both the normalization and shapes are taken from simulation. Contributions from events with misidentified leptons or leptons originating from the decay of b-hadrons or c-hadrons are estimated from data as described in Ref. [30].

The Monte Carlo samples which have been used for background processes are the same as those described in detail in Ref. [30]. A summary of the samples used to compute the central values of predicted background yields is reported in Table 1; additional samples are used in the evaluation of systematic uncertainties. The most accurate calculation of the total cross section for each process is used in the normalization of the samples in all cases, more details are reported in Ref. [30].

Signal samples with a top squark that always decays as $\tilde{t}_1 \to \nu_\tau b\tilde{\tau}_1 \to \nu_\tau b\tau\tilde{G}$ are generated with HERWIG++2.5.2 [40]. The top squark and the τ slepton mixings are such that the states involved in the

[1] ATLAS uses a right-handed coordinate system with its origin at the nominal interaction point (IP) in the centre of the detector and the z-axis coinciding with the axis of the beam pipe. The x-axis points from the IP to the centre of the LHC ring, and the y-axis points upwards. Cylindrical coordinates (r, ϕ) are used in the transverse plane, ϕ being the azimuthal angle around the beam pipe. The pseudorapidity is defined in terms of the polar angle θ as $\eta = -\ln\tan(\theta/2)$.

decay chain correspond to the partners of the corresponding right-handed SM fermions. The gravitino is assumed to be light enough that the τ slepton lifetime is at least two orders of magnitude shorter than the τ lepton lifetime. Signal cross sections are calculated to NLO in perturbative QCD, including the resummation of soft gluon emission at next-to-leading-logarithmic accuracy (NLO+NLL) [41–43], as described in Ref. [44]. Signal models have been generated for top squark mass values between 150 and 500 GeV, since models with smaller top squark mass values are expected to be excluded by previous searches [45, 46]. The τ slepton mass values range from the LEP limit at 87 GeV [22–26] to 490 GeV.

4 Physics object reconstruction

The same object definitions as Ref. [30] are used. Here only a brief summary of the identification criteria and kinematic selections is given for jets, leptons and transverse missing momentum.

Multiple vertex candidates from the proton–proton interaction are reconstructed using the tracks in the inner detector. The vertex with the highest scalar sum of the transverse momentum squared, Σp_{T}^2, of the associated tracks is defined as the primary vertex.

Jets are reconstructed from three-dimensional energy clusters in the calorimeter using the anti-k_t jet algorithm [47, 48] with a radius parameter of 0.4. Only jet candidates with $p_{\mathrm{T}} > 20$ GeV, $|\eta| < 2.5$ are retained. The inner detector tracking information is used to reject jets produced by pile-up interactions and to identify jets originating from b-quarks, referred to as b-jets in the following.

A neural-network-based algorithm is used to identify b-jets. The inputs to this algorithm are the impact parameter of inner detector tracks, the parameters of reconstructed secondary vertices and the topology of b- and c-hadron decays inside a jet [49]. The chosen operating point has an efficiency of 70% for tagging b-jets in a MC sample of $t\bar{t}$ events and rejection factors of 137 and 5 against jets originating from light quarks and c-quarks, respectively. To compensate for differences between the performance of the tagging algorithm in data and MC simulation, correction factors derived using $t\bar{t}$ events are applied to the jets in the simulation as described in Ref. [50].

Electron candidates are required to have $p_{\mathrm{T}} > 10$ GeV, $|\eta| < 2.47$ and to satisfy "tight" quality criteria [51] on the calorimetric and tracking measurements which discriminate electrons from jets. Non prompt and misidentified electrons are then suppressed by requiring the electrons to be isolated.

Muon candidates are reconstructed either from muon segments matched to inner detector tracks, or from combined tracks in the inner detector and muon spectrometer [52]. They are required to have $p_{\mathrm{T}} > 10$ GeV, $|\eta| < 2.4$. Muons from non collision sources, misidentified and non prompt muons are suppressed by requirements on the impact parameter from the reconstructed primary proton-proton interaction vertex, by the number of hits associated to various detectors, and by isolation requirements.

The measurement of the missing transverse momentum $\mathbf{p}_{\mathrm{T}}^{\mathrm{miss}}$, whose magnitude is referred to as $E_{\mathrm{T}}^{\mathrm{miss}}$, is based on the transverse momenta of all jets and lepton candidates and all calorimeter clusters not associated to these objects [53].

5 Event selection

5.1 Event preselection requirements

The new selection shares the same preselection requirements as Ref. [30]. Events are required to have exactly two opposite-sign (OS) leptons (electrons or muons). At least one electron or muon must have a momentum larger than 25 GeV, in order to be in the trigger efficiency plateau regions, and the invariant mass of the two leptons is required to be larger than 20 GeV. If the event contains a third preselected electron or muon, the event is rejected. In order to reduce the number of background events containing two leptons produced by the on-shell decay of the Z boson, the invariant mass of the same-flavour

lepton pairs is required to be outside the 71 − 111 GeV range. The angle $\Delta\phi(\mathbf{p}_{\mathrm{T}}^{\mathrm{miss}}, \mathbf{p}_{\mathrm{Tb}}^{\ell\ell})$ between the $\mathbf{p}_{\mathrm{T}}^{\mathrm{miss}}$ vector and the $\mathbf{p}_{\mathrm{Tb}}^{\ell\ell} = \mathbf{p}_{\mathrm{T}}^{\mathrm{miss}} + \mathbf{p}_{\mathrm{T}}^{\ell_1} + \mathbf{p}_{\mathrm{T}}^{\ell_2}$ vector[2], introduced in Ref. [54], is required to be smaller than 1.5. The azimuthal angle difference between the $\mathbf{p}_{\mathrm{T}}^{\mathrm{miss}}$ vector and the direction of the closest jet, $\Delta\phi(\mathbf{p}_{\mathrm{T}}^{\mathrm{miss}}$, closest jet), is required to be larger than 1.0.

5.2 Large $m_{\mathrm{T2}}^{\ell\ell}$ selection

Seven signal regions (SRs) constructed by further selections on the number of jets and the $m_{\mathrm{T2}}^{\ell\ell}$ variable, illustrated in Figure 2, were defined in the search reported in Ref. [30]. Their statistical combination is used to place limits on the GMSB top squark model.

The $m_{\mathrm{T2}}^{\ell\ell}$ variable is calculated as

$$m_{\mathrm{T2}}(\mathbf{p}_{\mathrm{T},1}, \mathbf{p}_{\mathrm{T},2}, \mathbf{p}_{\mathrm{T}}^{\mathrm{miss}}) = \min_{\mathbf{q}_{\mathrm{T},1}+\mathbf{q}_{\mathrm{T},2}=\mathbf{p}_{\mathrm{T}}^{\mathrm{miss}}} \{\max[\, m_{\mathrm{T}}(\mathbf{p}_{\mathrm{T},1}, \mathbf{q}_{\mathrm{T},1}), m_{\mathrm{T}}(\mathbf{p}_{\mathrm{T},2}, \mathbf{q}_{\mathrm{T},2})\,]\}, \tag{1}$$

where m_{T} indicates the transverse mass, $\mathbf{p}_{\mathrm{T},1}$ and $\mathbf{p}_{\mathrm{T},2}$ are the transverse momentum vectors of the two leptons, and $\mathbf{q}_{\mathrm{T},1}$ and $\mathbf{q}_{\mathrm{T},2}$ are transverse vectors which satisfy $\mathbf{q}_{\mathrm{T},1} + \mathbf{q}_{\mathrm{T},2} = \mathbf{p}_{\mathrm{T}}^{\mathrm{miss}}$. The minimisation is performed over all the possible decompositions of $\mathbf{p}_{\mathrm{T}}^{\mathrm{miss}}$.

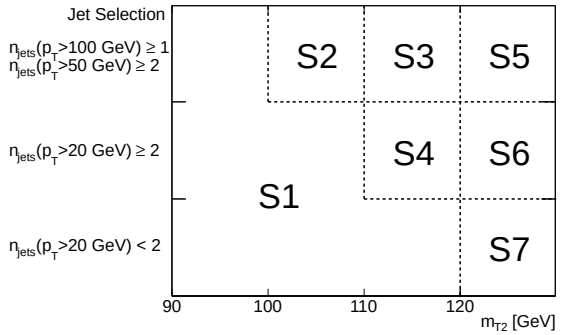

Figure 2: Scheme of the signal region definition in the (jet selections, $m_{\mathrm{T2}}^{\ell\ell}$) plane.

For the WW, Wt, and $t\bar{t}$ backgrounds, where the leptons and the undetected neutrinos are produced by the decays of W bosons, this variable is bounded from above by the W boson mass. For signal the two leptons and the undetected neutrinos and gravitinos are produced by the top squark decay, so this variable extends up to the top squark mass. In Figure 3 the fraction of signal which is selected by one of the SRs is shown as a function of the top squark and τ slepton masses. The selection efficiency increases with increasing values of both masses.

5.3 Small $m_{\mathrm{T2}}^{j\ell}$ selection

For small top squark and τ slepton masses, the sensitivity of the large $m_{\mathrm{T2}}^{\ell\ell}$ selections from Ref. [30] is very low despite the high production cross section. In order to recover sensitivity to such a signal, a new dedicated signal selection has been designed.

After the preselection, at least two jets with $p_T > 20$ GeV are required, at least one of them passing the b-tagging identification criteria. After this request the dominant SM background is $t\bar{t}$ production. The variable defined in Eq. 1 is then constructed using the $\mathbf{p}_{\mathrm{T},1} = (\mathbf{p}(\ell_1) + \mathbf{p}(j_1))_T$ and $\mathbf{p}_{\mathrm{T},2} = (\mathbf{p}(\ell_2) + \mathbf{p}(j_2))_T$

[2]Note that the b in $\mathbf{p}_{\mathrm{Tb}}^{\ell\ell}$ does not bear any relation to b-jet. In Ref. [54] it was so named to indicate that it represents the transverse momentum of boosted objects.

where ℓ_1, ℓ_2 are the two leptons and j_1, j_2 are two jets, selected as described below and denoted $m_{\mathrm{T2}}^{j\ell}$. If two or more jets in the event are tagged as b-jets, the two with the highest p_{T} are considered. If only one jet passes b-tagging requirements, the non-tagged jet with the highest b-tagging neural-network output value is considered. In order to pair each lepton with the jet coming from the same decay leg, the invariant mass ($m_{\ell j}$) is used. For background from top quark pair production, the kinematic end-point of $m_{\ell j}$ is about 155 GeV for the correct pairing. The signal models that are targeted have top squark mass values that range from 150 to 200 GeV: therefore the kinematic end-point of $m_{\ell j}$ is similar to that of the top pair background. Hence, only the lepton-jet combinations with invariant mass below 180 GeV are considered. If only one combination satisfies this request, this is taken and used for the calculation of the $m_{\mathrm{T2}}^{j\ell}$. If both combinations satisfy this request, the $m_{\mathrm{T2}}^{j\ell}$ is calculated for both combinations and the minimum is taken. If none of the combinations satisfies this request, the event is discarded.

The value of $m_{\mathrm{T2}}^{j\ell}$ is bounded from above by the top mass for the top pair background and by the top squark mass for signal. The $m_{\mathrm{T2}}^{j\ell}$ spectrum also peaks at smaller values, relative to the end-point, for the signal because more invisible particles are involved in the decay [55]. These features are illustrated in Figure 4, where the $m_{\mathrm{T2}}^{j\ell}$ distribution is reported for a signal with $\mathrm{m}_{\tilde{t}} = 153$ GeV and $\mathrm{m}_{\tilde{\tau}_1} = 117$ GeV, the top pair background and other SM backgrounds. An upper limit on $m_{\mathrm{T2}}^{j\ell}$ enhances the signal to background ratio for signals with a top squark mass smaller than or around the top quark mass. Signal candidates are required to have $m_{\mathrm{T2}}^{j\ell} < 70$ GeV, this value has been chosen by maximising the expected sensitivity. This selection enhances the contribution of the Z+jets background and of events with misidentified or non-prompt leptons, but $t\bar{t}$ production remains the dominant background.

Additional selections have been adopted to increase the sensitivity. The ratio $H_{\mathrm{T}}/m_{\mathrm{eff}}$ is required to be less than 0.4, where H_{T} is the scalar sum of the transverse momenta of the two leading jets, and m_{eff} is the scalar sum of the transverse momenta of the two leading jets, the transverse momenta of the leptons, and the missing transverse momentum. In addition to this, the ratio between $E_{\mathrm{T}}^{\mathrm{miss}}$ and the scalar sum of $E_{\mathrm{T}}^{\mathrm{miss}}$ plus the transverse momenta of the two leptons is required to be greater than 0.45. These two requirements enhance the sensitivity because the signal is characterized by higher missing transverse momentum, softer jets and softer leptons than the SM background.

Finally the absolute value of Δx is required to be less than 0.04, with Δx defined as:

$$\Delta x = \frac{2 \cdot (p_z^{\ell_1} + p_z^{\ell_2})}{\sqrt{(s)}}, \tag{2}$$

where $p_z^{\ell_1(\ell_2)}$ is the z component of the momentum of the leading (sub-leading) lepton and s is the center-of-mass energy in the proton-proton system. This quantity has been suggested in Ref. [56] in the context of the search for new particles via spin measurements. It has been found to have a good discrimination power and the selection requirement has been chosen by maximizing the expected sensitivity to the targeted scenarios.

The summary of the selection requirements is reported in Table 2.

6 Background estimation

The background estimate for the search of top squark pair production in events with large $m_{\mathrm{T2}}^{\ell\ell}$ is described in Ref. [30]. In this section, the estimate of the background contribution for the new small $m_{\mathrm{T2}}^{j\ell}$ signal region is discussed.

The dominant SM background contributions are top pair and Z+jets production. Following the approach described in Ref. [30], these background sources are evaluated by means of a likelihood fit with the observed events in two data control regions (CRs) as constraints and the normalisation terms for each background as free parameters. The two control regions are defined as:

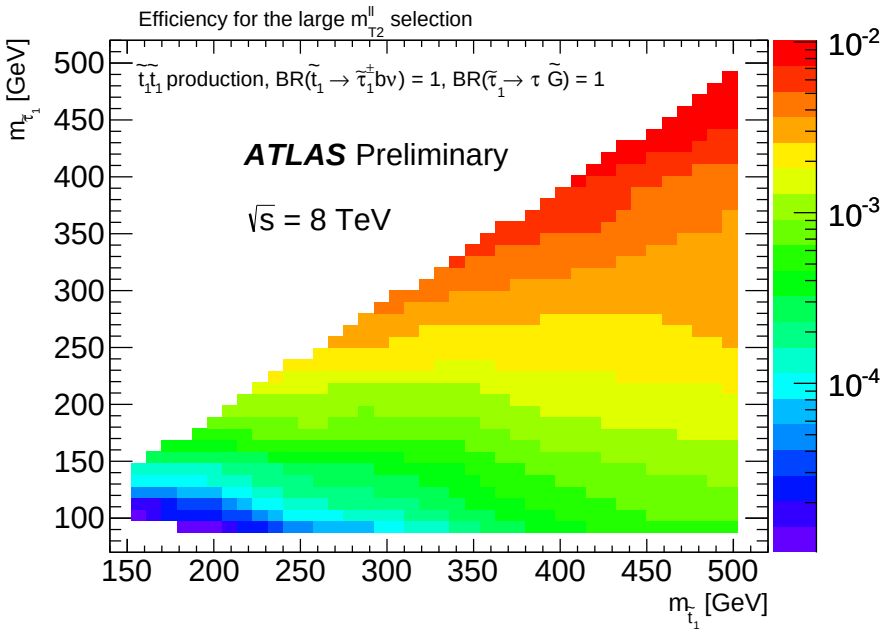

Figure 3: Efficiency of large $m_{\mathrm{T2}}^{\ell\ell}$ selection: fraction of signal events that are selected by at least one SR of Ref. [30] as a function of top squark and τ slepton masses.

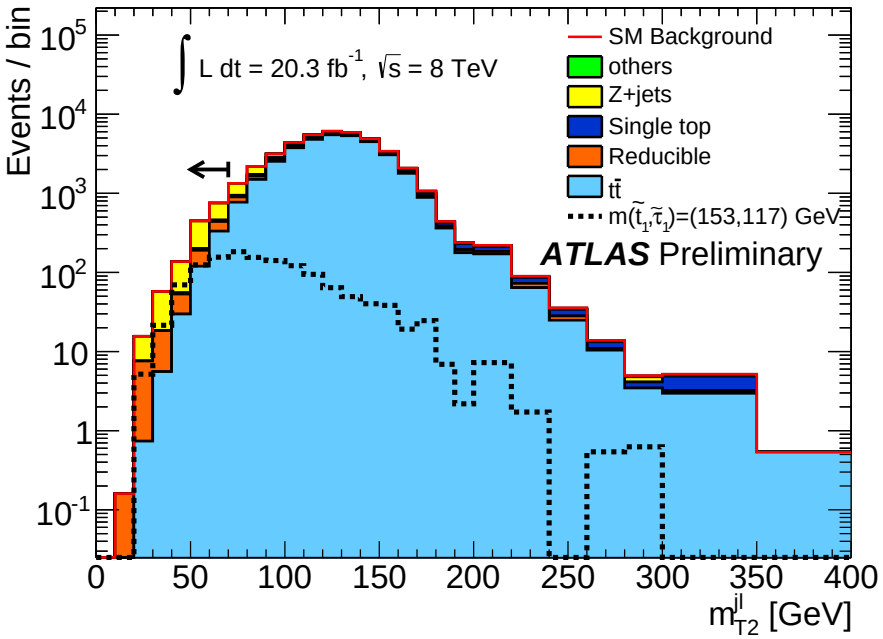

Figure 4: Distribution of $m_{\mathrm{T2}}^{j\ell}$ for the total SM background, the top pair background and a signal model with $m_{\tilde{t}_1}$ = 153 GeV and $m_{\tilde{\tau}_1}$ = 117 GeV, after the preselection and the selection of the jets described in the text. The black arrow marks the selection used to define the new signal region.

Preselection	
p_{T} leading lepton	> 25 GeV
p_{T} sub-leading lepton	> 10 GeV
$m(\ell\ell)$	$e\mu : > 20$ GeV
	$ee, \mu\mu : 20 < m(\ell\ell) < 71$ GeVor $m(\ell\ell) > 111$ GeV
$\Delta\phi(\mathbf{p}_{\mathrm{T}}^{\mathrm{miss}}$, closest jet)	> 1.0
$\Delta\phi(\mathbf{p}_{\mathrm{T}}^{\mathrm{miss}}, \mathbf{p}_{\mathrm{Tb}}^{\ell\ell})$	< 1.5
Small $m_{\mathrm{T2}}^{j\ell}$ selection	
jets with $p_{\mathrm{T}} > 20$ GeV	≥ 2
b-jets with $p_{\mathrm{T}} > 20$ GeV	≥ 1
$m_{\mathrm{T2}}^{j\ell}$	< 70 GeV
$H_{\mathrm{T}}/m_{\mathrm{eff}}$	< 0.4
$E_{\mathrm{T}}^{\mathrm{miss}}/(E_{\mathrm{T}}^{\mathrm{miss}}$ + lepton momenta)	> 0.45
$\lvert\Delta x\rvert$	< 0.04

Table 2: Summary of the signal region selections for small top squark and τ slepton masses.

- **CRTb**, defined by different flavour (eμ) events with 80 GeV $< m_{\mathrm{T2}}^{j\ell} <$ 100 GeV and passing all the SR selection requirements on other variables as described in Section 5.
- **CRZb**, defined by same flavour (ee or $\mu\mu$) events which have $m_{\mathrm{T2}}^{j\ell} < 70$ GeV and pass all the preselection requirements apart for the veto on the Z mass window. This requirement is reversed and the two-lepton invariant mass is required to be between 71 GeV and 111 GeV. Events are then required to have at least 2 jets, one of them tagged as a b-jet and $H_{\mathrm{T}}/m_{\mathrm{eff}}$ <0.4.

Figure 5 shows the distribution of $m_{\mathrm{T2}}^{j\ell}$ for different flavour events passing all the selections of CRTb except that on $m_{\mathrm{T2}}^{j\ell}$ itself and the distribution of $m_{\mathrm{T2}}^{j\ell}$ for same flavour events passing all the selections of CRZb except that on $m_{\mathrm{T2}}^{j\ell}$ itself.

Additional SM processes yielding two isolated leptons and $E_{\mathrm{T}}^{\mathrm{miss}}$ (dibosons, Higgs, Wt, $t\bar{t}W$ and $t\bar{t}Z$), and providing a sub-dominant contribution to the SR are determined from MC simulation. The non-prompt and misidentified lepton background is estimated from data using the same method described in Ref. [30].

The result of the fit as well as the expected background composition before the fit are reported in Table 3. For the $t\bar{t}$ and Z+jets backgrounds the fraction of events where at least one lepton comes from τ decays is reported. For the top pair background, the expected contribution of events with a τ in the signal region is very similar to that in the control region. For the Z background the contribution is expected to be very different between the control region and the signal region. No events with a τ enter in the control region, while the contribution in the signal region is about 50%.

The fit uses the same normalization factors for $Z(ee)$, $Z(\mu\mu)$, and $Z \to \tau\tau \to \ell\nu_\ell\nu_\tau\ell\nu_\ell\nu_\tau$. In order to verify that the MC correctly describes the ratio of event yields between these processes, and thus a common normalization factor can be used, an auxiliary fit is performed. A validation region (VR), composed of $e\mu$ events passing the preselection and containing at least two jets, no b-tagged jet, $m_{\mathrm{T2}}^{\ell\ell} <$ 15 GeV, and $m(\ell\ell) < 80$ GeV, is defined. The $Z(\tau\tau)$+jets events are 58% of the total expected events in this region, while the expected rate from $Z(\ell\ell)$+jets is negligible. The Z+jets normalization for this auxiliary fit is derived with a control region using the same selections as VRZ, except that same flavour events with 71 GeV $< m(\ell\ell) <$ 111 GeV are required. The control and validation regions used in the auxiliary fit are defined in Table 4, where the observed number of events and the fitted background are reported. A good agreement is observed in the validation region between data and the predicted

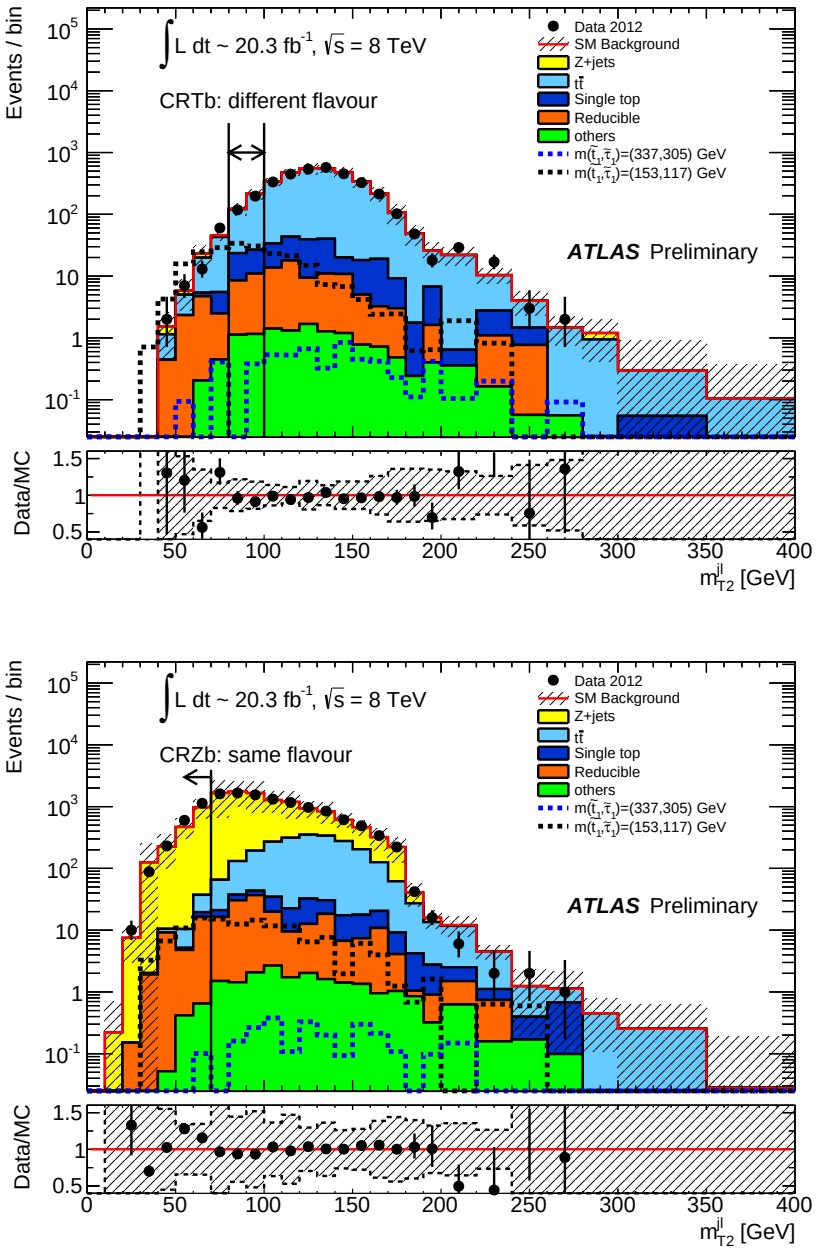

Figure 5: Distribution of the $m_{\mathrm{T2}}^{j\ell}$ variable for different flavour events passing all the selections of CTRb apart for the selection on $m_{\mathrm{T2}}^{j\ell}$ itself (top) and for events with two same flavour isolated leptons passing all the selections of CRZb apart for the selection on $m_{\mathrm{T2}}^{j\ell}$ itself (bottom). The components labelled "Reducible" are the events with misidentified or non-prompt leptons and they are estimated from data as described in Ref. [30]; the other backgrounds are estimated from MC simulation, normalized to the theoretical cross section. The expected distributions for two signal models are also shown: the black dashed line corresponds to a model with m($\tilde{t}_1$)=153 GeV, m($\tilde{\tau}_1$)=117 GeV; the blue dashed line to a model with m($\tilde{t}_1$)=337 GeV, m($\tilde{\tau}_1$)=305 GeV. The term "others" includes dibosons, Higgs and ttV contributions. Combined statistical, experimental and theoretical systematic uncertainties are included in the error bands. The black lines and the arrows mark the selection values used to define the control regions.

Table 3: Results of the background determination from fits to the two control regions. The total expected background is computed using the normalizations from the fit and it is constrained to be equal to the observed number of events in the control regions. Nominal background expectations (normalized to the theoretical cross section) are given for comparison for those backgrounds (top pair and Z+jets production) which are normalized to data. Combined statistical, experimental and theoretical systematic uncertainties are included. Events with misidentified or non-prompt leptons are estimated with the data-driven technique described in Ref. [30]. The term "MC other backgrounds" includes dibosons, Higgs and ttV contributions. (*): In the control regions the fitted background events correspond to the observed events with their statistical uncertainty.

channel	CRTb	CRZb
Observed events	315	2061
Fitted bkg events (*)	315 ± 18	2061 ± 50
Fitted Top events	258 ± 24	22 ± 4
Fitted $Z(ee, \mu\mu, \tau\tau)$ events	7 ± 6	2000 ± 50
MC exp. SM events	340 ± 70	1800 ± 700
MC exp. Top events	280 ± 60	24 ± 8
τ contribution	29%	21%
MC exp. $Z(ee, \mu\mu, \tau\tau)$ events	6^{+7}_{-6}	1700 ± 700
τ contribution	95%	< 1%
MC exp. Wt events	31 ± 10	$3.5^{+3.9}_{-3.5}$
MC other backgrounds	$2.3^{+1.7}_{-1.6}$	$1.1^{+1.7}_{-1.1}$
data-driven expected misidentified/non-prompt leptons	17 ± 7	31 ± 16

Table 4: Definition of the regions used in the auxiliary fit, and fit results. The errors shown are the statistical plus systematic uncertainties. (*): In the control regions the fitted background events correspond to the observed events with their statistical uncertainty.

channel	CRTb	CRZ	VR
Flavour	$e\mu$	ee and $\mu\mu$	$e\mu$
$m(\ell\ell)$	> 20 GeV	71 GeV < $m(\ell\ell)$ < 111 GeV	< 80 GeV
jets with p_{T} > 20 GeV	≥ 2	≥ 2	≥ 2
b-jets with p_{T} > 20 GeV	≥ 1	0	0
$m^{\ell\ell}_{\mathrm{T2}}$	no requirement	< 15 GeV	< 15 GeV
$m^{j\ell}_{\mathrm{T2}}$	80 GeV < $m^{j\ell}_{\mathrm{T2}}$ < 100 GeV	no requirement	no requirement
$H_{\mathrm{T}}/m_{\mathrm{eff}}$	< 0.4	no requirement	no requirement
$E^{\mathrm{miss}}_{\mathrm{T}}/(E^{\mathrm{miss}}_{\mathrm{T}}$ + lepton momenta)	> 0.45	no requirement	no requirement
$\lvert\Delta x\rvert$	< 0.04	no requirement	no requirement
Observed events	315	277557	5879
Fitted bkg events (*)	315 ± 18	277557 ± 500	6100 ± 500

background, showing that the same normalization can indeed be used for $Z(ee)$, $Z(\mu\mu)$, and $Z \to \tau\tau \to \ell\nu_\ell\nu_\tau\ell\nu_\ell\nu_\tau$ as done for the SR fit.

The description of the background coming from misidentified or non-prompt leptons has been tested as well, since its contribution in the new signal region is significant. A sample enriched with misidentified or non-prompt leptons has been selected by requiring the presence of two same sign leptons. Events have then been required to pass all the preselection requirements, to have at least two jets, one of them b-tagged, and $m_{jl} < 180$ GeV. Figure 6 shows the distribution of $m_{\mathrm{T2}}^{j\ell}$ for the different flavour and the same flavour channels separately. The predictions are in agreement with the data within the uncertainty.

7 Systematic Uncertainties

The estimate of the various sources of systematic uncertainties follows the same procedure as in Ref. [30].

For the experimental systematic uncertainties, non-negligible contributions are due to the jet energy scale (JES) and the jet energy resolution (JER) uncertainties and the uncertainty on the b-tagging efficiency. Additional uncertainties arise from the contribution to $E_{\mathrm{T}}^{\mathrm{miss}}$ from the energy scale and resolution of the calorimeter cells not associated to electrons, muons or jets, and also from low momentum (7 GeV $< p_{\mathrm{T}} <$ 25 GeV) jets. The uncertainties in the lepton reconstruction efficiency and in the trigger modeling and on the modeling of pile-up have a negligible impact on the analysis. A ±2.8% uncertainty on the luminosity determination was measured using techniques similar to those described in Ref. [57] from a preliminary calibration of the luminosity scale derived from beam-separation scans performed in November 2012. It is included for all signal and background MC simulations.

The uncertainty on the misidentified or non-prompt lepton background estimate has been calculated as in Ref. [30] and it is the 1.5% of the total background uncertainty in the SR.

The leading theoretical uncertainties are due to the modeling of the Z+jets background, evaluated comparing the predictions of `SHERPA` and `ALPGEN`, and of the top pair background, evaluated comparing the predictions of `MC@NLO` and `POWHEG` for the matrix element calculation, the predictions of `PYTHIA` and `Herwig` for the parton showering and hadronization, and the predictions of two `ACERMC` samples with different tunings for the uncertainties related to the amount of initial and final state radiation (ISR and FSR).

Other significant sources of uncertainty are the limited number of events in the CRs and MC simulation samples.

A summary of the uncertainties on the total expected background for the new small $m_{\mathrm{T2}}^{j\ell}$ signal region is given in Table 5. The row labelled "samples size" includes the effects of the limited number of data events in the CRs and the limited number of MC simulated events.

Experimental systematic uncertainties are also evaluated for the expected signal yields. They are about 30% for the targeted SUSY models, and are dominated by the JER uncertainty. The uncertainty on the signal cross section predictions is calculated as in Ref. [30] and the typical cross section uncertainty is ±15% for the top squark signals considered in this search.

8 Results

Figure 7 shows the distributions of the $m_{\mathrm{T2}}^{j\ell}$ variable after applying all the selection criteria except that on $m_{\mathrm{T2}}^{j\ell}$. For illustration, the distributions for two signal models are also shown. The data agree with the SM background expectation within uncertainties.

Table 6 shows the expected number of events in the new small $m_{\mathrm{T2}}^{j\ell}$ SR for each background source and the observed numbers of events. No excess of events is observed in data. Upper limits at 95% CL on the number of beyond the SM (BSM) events are derived using the CLs prescription [58] and neglecting

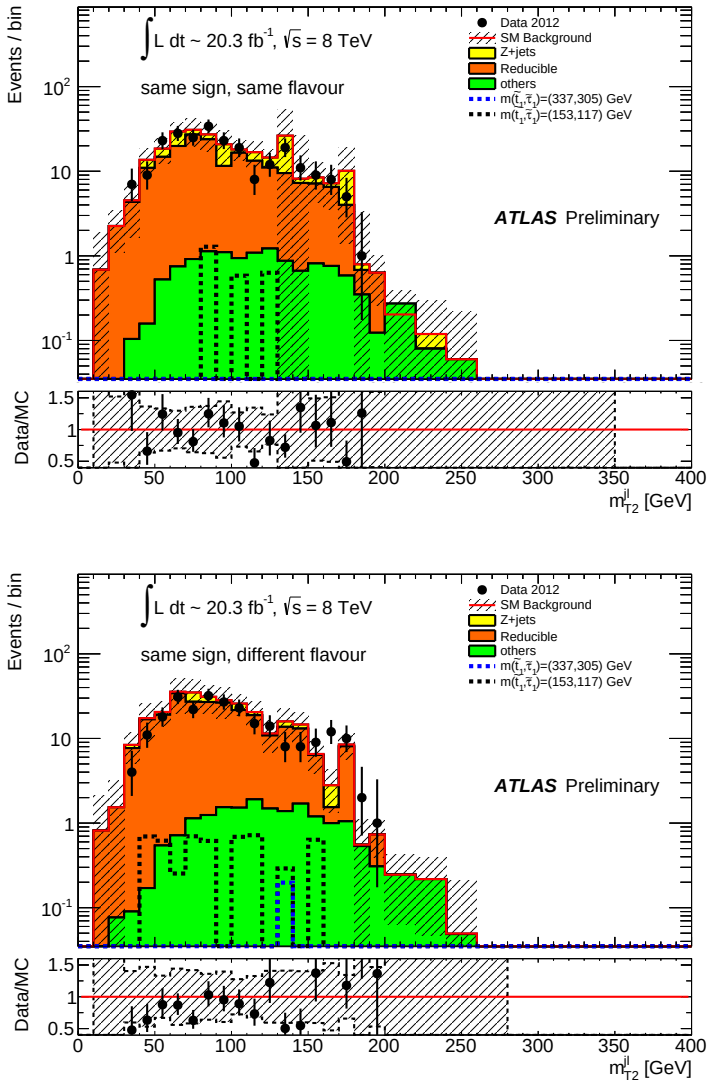

Figure 6: Distribution of $m_{\mathrm{T2}}^{j\ell}$ for events with two same sign isolated leptons, passing all the preselection requirements, the request of the presence of at least 2 jets (one of them b-tagged) and $\mathrm{m}_{j\ell} < 180$ GeV. The components labelled "Reducible" are the events with misidentified or non-prompt leptons and they are estimated from data as described in Ref. [30]; the other backgrounds are estimated from MC simulation. The expected distributions for two signal models are also shown: the black dashed line corresponds to a model with $\mathrm{m}(\tilde{t}_1)$=153 GeV, $\mathrm{m}(\tilde{\tau}_1)$=117 GeV; the blue dashed line to a model with $\mathrm{m}(\tilde{t}_1)$=337 GeV, $\mathrm{m}(\tilde{\tau}_1)$=305 GeV. The term "others" includes dibosons, Higgs and ttV contributions. The plots report the distribution for the same flavour (top) and different flavour (bottom) channel respectively. Combined statistical, experimental and theoretical systematic uncertainties are included in the error bands.

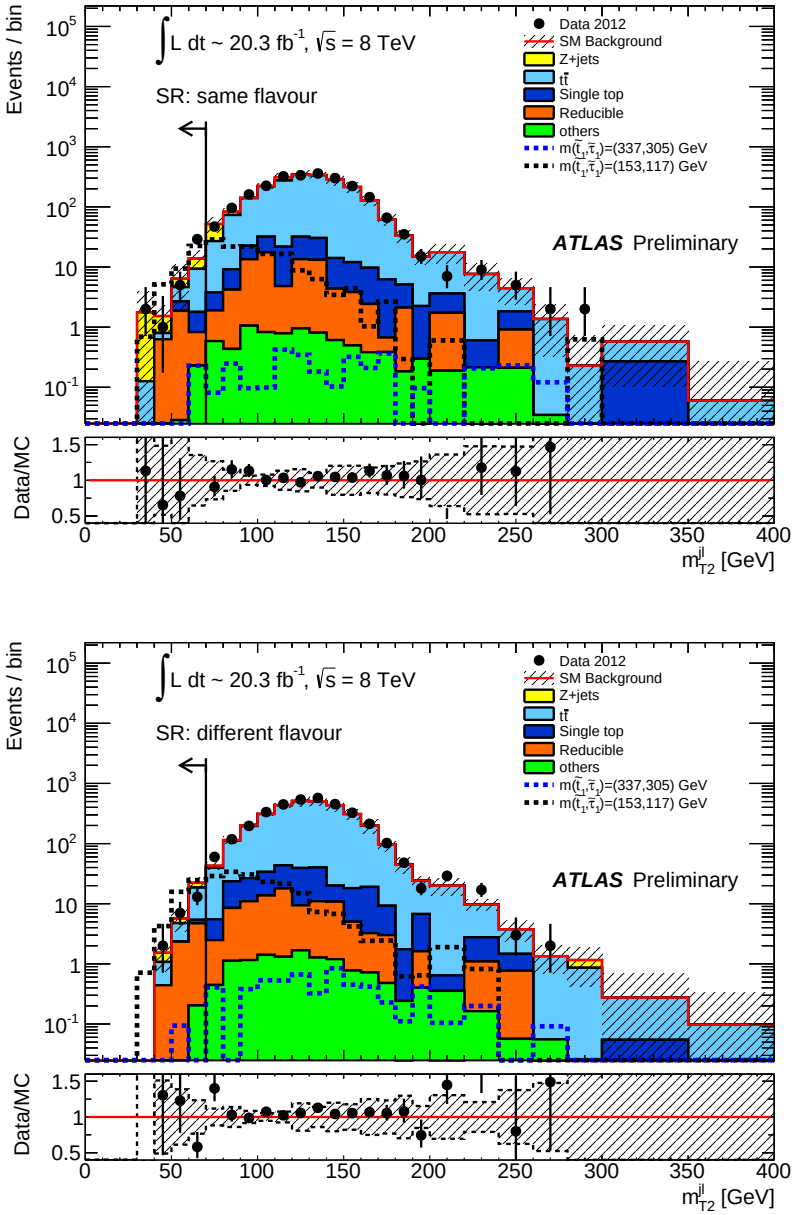

Figure 7: Distributions of $m_{\mathrm{T2}}^{j\ell}$ for events passing all the signal candidate selection requirements, except that on $m_{\mathrm{T2}}^{j\ell}$ for (top) same flavour and (bottom) different flavour events. The contributions from all SM backgrounds are shown; the bands represent the total uncertainty, including combined statistical, experimental and theoretical systematic uncertainties. The components labelled "Reducible" are the events with misidentified or non-prompt leptons and they are estimated from data as described in Ref. [30]; the other backgrounds are estimated from MC simulation with normalizations measured in control regions described in Section 6 for $t\bar{t}$ and Z+jets backgrounds. The expected distributions for two signal models are also shown: the black dashed line corresponds to a model with m($\tilde{t}_1$)=153 GeV, m($\tilde{\tau}_1$)=117 GeV; the blue dashed line to a model with m($\tilde{t}_1$)=337 GeV, m($\tilde{\tau}_1$)=305 GeV. The term "others" includes dibosons, Higgs and ttV contributions. The black lines and the arrows mark the selection value used to define the new signal region.

Table 5: Systematic uncertainties on the background estimate in the new small $m_{\mathrm{T2}}^{j\ell}$ signal region: the variations in the predicted background yield are quoted. The uncertainties on $t\bar{t}$ normalization and Z+jets normalization include the uncertainties in the control regions, while the top modeling uncertainty includes generator, parton shower and ISR/FSR uncertainties. It should be noted that the individual uncertainties can be correlated.

Source	Uncertainty [%]
cluster energy scale and resolution	11
sample size	9
top modeling	7
$t\bar{t}$ normalization	5
jet energy scale and resolution	4
top ISR/FSR	3
fake or non-prompt lepton uncertainties	3
Z+jets normalization	2
b-tagging	1
Z+jets modeling	1
Total uncertainty	20

Table 6: Number of events observed in 20.3 fb^{-1} of data at 8 TeV centre-of-mass energy, in the signal region, compared with background expectations obtained from the fits described in the text. The expectations (normalised to theoretical cross-sections) are given for comparison for those backgrounds (top pair and Z+jets production) which are normalized to data. Combined statistical, experimental and theoretical systematic uncertainties are indicated. The term "MC other backgrounds" includes dibosons, Higgs and ttV contributions.

channel	SR
Observed events	59
Fitted bkg events	53 ± 10
Fitted Top events	26 ± 5
Fitted $Z(ee, \mu\mu, \tau\tau)$ events	14 ± 7
MC exp. SM events	54 ± 14
MC exp. Top events	29 ± 8
τ contribution	32%
MC exp. $Z(ee, \mu\mu, \tau\tau)$ events	12 ± 7
τ contribution	52%
MC exp. Wt events	2.5 ± 2.0
MC other backgrounds	$0.47^{+0.51}_{-0.39}$
data-driven exp. misidentified/non-prompt leptons	10.0 ± 3.5

Table 7: Upper limit on the visible cross section σ_{vis} in the new small $m_{\text{T2}}^{j\ell}$ SR, using toy MC pseudo experiments and an asymptotic method [59].

	σ_{obs}[fb]	S_{obs} [events]	S_{exp} [events]	CL_b	p(s=0)
Pseudo experiments	1.49	30.2	27^{+8}_{-6}	0.69	0.32
Asymptotics	1.48	30.1	26^{+10}_{-7}	0.68	0.32

any possible contamination in the control regions. Normalizing these by the integrated luminosity of the data sample they can be interpreted as upper limits on the visible BSM cross-section, σ_{vis}. Where σ_{vis} is defined as the product of acceptance, reconstruction efficiency and production cross-section. The results are given in Table 7 for the new small $m_{\text{T2}}^{j\ell}$ signal region.

The results obtained are used to derive the model dependent limits on the mass of a pair-produced top squark $\tilde{t}_1$ decaying with 100% branching ratio into a b-quark, a $\tilde{\tau}_1$ and a neutrino, with the $\tilde{\tau}_1$ decaying into a τ and a gravitino. These limits take into account the uncertainties on the signal and the signal contamination in the control regions, which is of the order of 20% in CRTb and 2% in CRZb, considering the signal models for which this analysis has sensitivity.

In Figure 8 the expected (dashed line) and observed 95% C.L. limits are reported as a function of the top squark and τ slepton masses. For each signal point the selection that gives the best expected CL_s between the new signal region and the combination SRs defined in Ref. [30] has been considered. The new signal region is used for top squark masses below 200 GeV and mass differences between the top squark and the τ slepton greater than 10 GeV. The coloured band is the $\pm 1\sigma$ band around the expected limit. The dotted (red) lines around the observed limit represent the results obtained when moving the nominal signal cross-section up or down by its theoretical uncertainty.

SUSY models where the mass difference between the top squark and the τ slepton is below 35 GeV are excluded at 95% C.L. for top squark masses up to 480 GeV and masses below 170 GeV are excluded for each τ slepton mass value. Quoted numerical limits on the particle masses are taken from these -1σ "theory lines".

9 Conclusions

A search for a scalar partner of the top quark which decays into a τ slepton, a b-quark and a neutrino, with the τ slepton decaying into a τ lepton and a gravitino, has been performed using 20.3 fb^{-1}of pp collision data at $\sqrt{s} = 8$ TeV produced by the LHC and collected by the ATLAS detector. Sensitivity to the signal has been achieved by reinterpreting the results of a previous search [30] and performing a new search specifically targeting small $\tilde{t}_1$ and $\tilde{\tau}_1$ masses. For both analyses, the number of observed events in the signal region has been found to be consistent with the Standard Model expectations. Limits have then been derived on the mass of a supersymmetric scalar top and the τ slepton. A supersymmetric top squark $\tilde{t}_1$ with a mass lower than 170 GeV has been excluded at 95% CL for any value of the τ slepton mass, assuming that the decay chain described above occurs with 100% branching ratio. Under the same assumption, a top squark mass smaller than 480 GeV is excluded at 95% CL for a difference between the top squark and τ slepton masses smaller than 35 GeV.

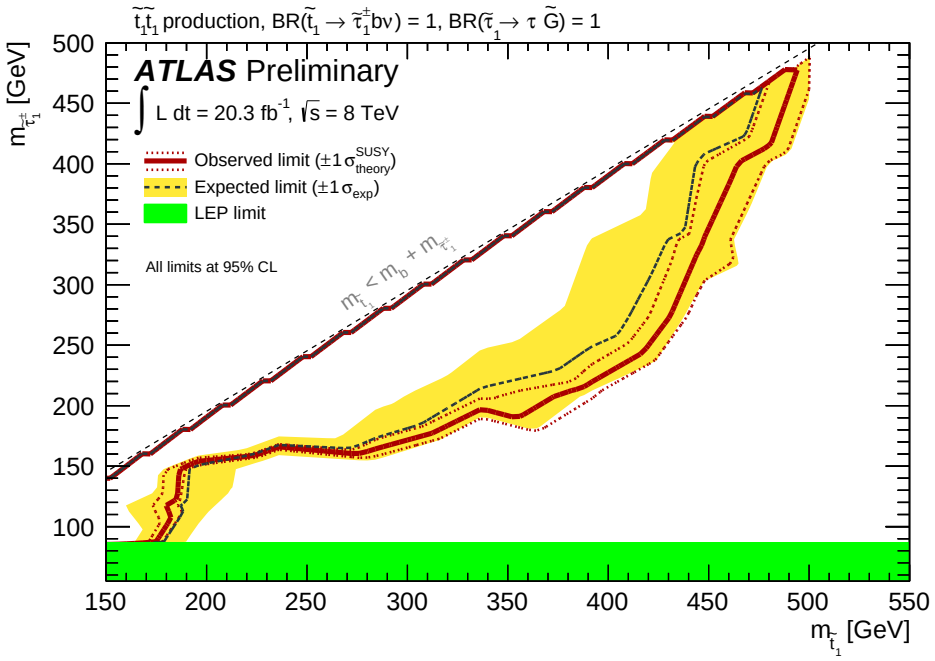

Figure 8: Exclusion limits at 95% CL from the analysis of 20.3 fb^{-1} of 8 TeV collision data on the masses of the top squark and $\tilde{\tau}_1$ and assuming BR($\tilde{t}_1 \to b\tilde{\tau}_1\nu$) = 1. The blue dashed line and the yellow band are the expected limit and its $\pm 1\sigma$ uncertainty, respectively. The thick solid line is the observed limit for the central value of the signal cross section. The dotted lines show the effect on the observed limit when varying the signal cross section by $\pm 1\sigma$ of the theoretical uncertainty. The green band represents the LEP limit [22–26] on the τ slepton mass.

References

[1] S. Weinberg, *Implications of Dynamical Symmetry Breaking*, Phys. Rev. **D13** (1976) 974.

[2] E. Gildener, *Gauge Symmetry Hierarchies*, Phys. Rev. **D14** (1976) 1667.

[3] S. Weinberg, *Implications of Dynamical Symmetry Breaking: An Addendum*, Phys. Rev. **D19** (1979) 1277.

[4] L. Susskind, *Dynamics of Spontaneous Symmetry Breaking in the Weinberg- Salam Theory*, Phys. Rev. **D20** (1979) 2619.

[5] L. Evans and P. Bryant, *LHC machine*, JINST **3** (2008) S08001.

[6] H. Miyazawa, *Baryon Number Changing Currents*, Prog. Theor. Phys. **36 (6)** (1966) 1266–1276.

[7] P. Ramond, *Dual Theory for Free Fermions*, Phys. Rev. **D3** (1971) 2415.

[8] Y. Golfand and E. Likhtman, *Extension of the Algebra of Poincare Group Generators and Violation of p Invariance*, JETP Lett. **13** (1971) 323.

[9] A. Neveu and J. H. Schwarz, *Factorizable dual model of pions*, Nucl. Phys. **B31** (1971) 86.

[10] A. Neveu and J. H. Schwarz, *Quark Model of Dual Pions*, Phys. Rev. **D4** (1971) 1109.

[11] J. L. Gervais and B. Sakita, *Field theory interpretation of supergauges in dual models*, Nucl. Phys. **B34** (1971) 632.

[12] D. L. Volkov and V. Akulov, *Is the Neutrino a Goldstone Particle?*, Phys. Lett. **B46** (1973) 109.

[13] J. Wess and B. Zumino, *A Lagrangian Model Invariant Under Supergauge Transformations*, Phys. Lett. **B49** (1974) 52.

[14] J. Wess and B. Zumino, *Supergauge Transformations in Four-Dimensions*, Nucl. Phys. **B70** (1974) 39.

[15] P. Fayet, *Supersymmetry and Weak, Electromagnetic and Strong Interactions*, Phys. Lett. **B64** (1976) 159.

[16] P. Fayet, *Spontaneously Broken Supersymmetric Theories of Weak, Electromagnetic and Strong Interactions*, Phys. Lett. **B69** (1977) 489.

[17] G. R. Farrar and P. Fayet, *Phenomenology of the Production, Decay, and Detection of New Hadronic States Associated with Supersymmetry*, Phys. Lett. **B76** (1978) 575.

[18] P. Fayet, *Relations Between the Masses of the Superpartners of Leptons and Quarks, the Goldstino Couplings and the Neutral Currents*, Phys. Lett. **B84** (1979) 416.

[19] S. Dimopoulos and H. Georgi, *Softly Broken Supersymmetry and SU(5)*, Nucl. Phys. **B193** (1981) 150.

[20] R. Barbieri and G. Giudice, *Upper Bounds on Supersymmetric Particle Masses*, Nucl.Phys. **B306** (1988) 63.

[21] M. Asano, H. D. Kim, R. Kitano, and Y. Shimizu, *Natural Supersymmetry at the LHC*, JHEP **1012** (2010) 019, `arXiv:1010.0692 [hep-ph]`.

[22] LEPSUSYWG, ALEPH, DELPHI, L3 and OPAL experiments LEPSUSYWG/04-01.1. http://lepsusy.web.cern.ch/lepsusy/www/sleptons_summer04/slep_final.html.

[23] OPAL Collaboration, *Searches for gauge-mediated supersymmetry breaking topologies in e+ e- collisions at LEP2*, Eur.Phys.J. **C46** (2006) 307–341, arXiv:hep-ex/0507048 [hep-ex].

[24] ALEPH Collaboration, *Search for scalar leptons in e+ e- collisions at center-of-mass energies up to 209-GeV*, Phys.Lett. **B526** (2002) 206–220, arXiv:hep-ex/0112011 [hep-ex].

[25] DELPHI Collaboration, *Searches for supersymmetric particles in e+ e- collisions up to 208-GeV and interpretation of the results within the MSSM*, Eur.Phys.J. **C31** (2003) 421–479, arXiv:hep-ex/0311019 [hep-ex].

[26] L3 Collaboration Collaboration, P. Achard et al., *Search for scalar leptons and scalar quarks at LEP*, Phys.Lett. **B580** (2004) 37–49, arXiv:hep-ex/0310007 [hep-ex].

[27] ATLAS Collaboration, *Search for direct production of the top squark in the all-hadronic $t\bar{t} + E_{\mathrm{T}}^{\mathrm{miss}}$ final state in 21 fb^{-1} of pp collisions at $\sqrt{s}$ = 8 TeV with the ATLAS detector.*, ATLAS-CONF-2013-024. http://cdsweb.cern.ch/record/1525880.

[28] ATLAS Collaboration, *Search for direct third-generation squark pair production in final states with missing transverse momentum and two b-jets in $\sqrt{s}$ = 8 TeV pp collisions with the ATLAS detector*, JHEP **1310** (2013) 189, arXiv:1308.2631 [hep-ex].

[29] ATLAS Collaboration, *Search for direct top squark pair production in final states with one isolated lepton, jets, and missing transverse momentum in $\sqrt{s}$ = 8 TeV pp collisions using 21 fb^{-1} of ATLAS data*, ATLAS-CONF-2013-037. http://cdsweb.cern.ch/record/1532431.

[30] ATLAS Collaboration, *Search for direct top-squark pair production in final states with two leptons in pp collisions at $\sqrt{s}$ = 8 TeV with the ATLAS detector*, arXiv:1403.4853 [hep-ex].

[31] ATLAS Collaboration, *The ATLAS Experiment at the CERN Large Hadron Collider*, JINST **3** (2008) S08003.

[32] G. Corcella et al., *HERWIG 6: An Event generator for hadron emission reactions with interfering gluons (including supersymmetric processes)*, JHEP **0101** (2001) 010, arXiv:hep-ph/0011363 [hep-ph].

[33] T. Sjostrand, S. Mrenna, and P. Z. Skands, *PYTHIA 6.4 Physics and Manual*, JHEP **0605** (2006) 026, arXiv:hep-ph/0603175 [hep-ph].

[34] T. Gleisberg et al., *Event generation with SHERPA 1.1*, JHEP **0902** (2009) 007, arXiv:0811.4622 [hep-ph].

[35] M. L. Mangano, M. Moretti, F. Piccinini, R. Pittau, and A. D. Polosa, *ALPGEN, a generator for hard multiparton processes in hadronic collisions*, JHEP **0307** (2003) 001, arXiv:hep-ph/0206293 [hep-ph].

[36] S. Frixione and B. R. Webber, *Matching NLO QCD computations and parton shower simulations*, JHEP **0206** (2002) 029, arXiv:hep-ph/0204244 [hep-ph].

[37] S. Frixione, E. Laenen, P. Motylinski, and B. R. Webber, *Single-top production in MC@NLO*, JHEP **03** (2006) 092, arXiv:hep-ph/0512250.

[38] J. Alwall, M. Herquet, F. Maltoni, O. Mattelaer, and T. Stelzer, *MadGraph 5 : Going Beyond*, JHEP **1106** (2011) 128, arXiv:1106.0522 [hep-ph].

[39] S. Frixione, P. Nason, and C. Oleari, *Matching NLO QCD computations with Parton Shower simulations: the POWHEG method*, JHEP **0711** (2007) 070, arXiv:0709.2092 [hep-ph].

[40] M. Bahr et al., *Herwig++ Physics and Manual*, Eur. Phys. J. **C58** (2008) 639, arXiv:0803.0883 [hep-ph]. 143 pages, program and additional information available from http://projects.hepforge.org/herwig.

[41] W. Beenakker, M. Kramer, T. Plehn, M. Spira, and P. M. Zerwas, *Stop production at hadron colliders*, Nucl. Phys. **B515** (1998) 3, hep-ph/9710451.

[42] W. Beenakker et al., *Supersymmetric top and bottom squark production at hadron colliders*, JHEP **1008** (2010) 098, arXiv:1006.4771 [hep-ph].

[43] W. Beenakker et al., *Squark and gluino hadroproduction*, Int. J. Mod. Phys. **A26** (2011) 2637, arXiv:1105.1110 [hep-ph].

[44] M. Kramer, A. Kulesza, R. van der Leeuw, M. Mangano, S. Padhi, T. Plehn, and X. Portell, *Supersymmetry production cross sections in pp collisions at* $\sqrt{s} = 7$ TeV, arXiv:1206.2892.

[45] ATLAS Collaboration, *Search for light scalar top quark pair production in final states with two leptons with the ATLAS detector in* $\sqrt{s} = 7$ *TeV proton-proton collisions*, arXiv:1208.4305 [hep-ex].

[46] ATLAS Collaboration, *Search for light top squark pair production in final states with leptons and b−jets with the ATLAS detector in* $\sqrt{s} = 7$ *TeV proton-proton collisions*, arXiv:1209.2102 [hep-ex].

[47] M. Cacciari and G. P. Salam, *Dispelling the* N^3 *myth for the* k_t *jet-finder*, Phys. Lett. **B641** (2006) 57, arXiv:hep-ph/0512210 [hep-ph].

[48] M. Cacciari, G. P. Salam, and G. Soyez, *The Anti-k(t) jet clustering algorithm*, JHEP **0804** (2008) 063, arXiv:0802.1189 [hep-ph].

[49] ATLAS Collaboration, *Commissioning of the ATLAS high-performance b-tagging algorithms in the 7 TeV collision data*, ATLAS-CONF-2011-102. http://cds.cern.ch/record/1369219.

[50] ATLAS Collaboration, *Measuring the b-tag efficiency in a top-pair sample with 4.7* fb^{-1} *of data from the ATLAS detector*, ATLAS-CONF-2012-097. https://cds.cern.ch/record/1460443.

[51] ATLAS Collaboration, *Electron performance measurements with the ATLAS detector using the 2010 LHC proton-proton collision data*, Eur. Phys. J. **C72** (2012) 1909, arXiv:1110.3174 [hep-ex].

[52] ATLAS Collaboration, *Muon reconstruction efficiency in reprocessed 2010 LHC proton-proton collision data recorded with the ATLAS detector*, ATLAS-CONF-2011-063. http://cdsweb.cern.ch/record/1345743.

[53] ATLAS Collaboration, *Performance of Missing Transverse Momentum Reconstruction in Proton-Proton Collisions at 7 TeV with ATLAS*, Eur. Phys. J. **C72** (2012) 1844, arXiv:1108.5602 [hep-ex].

[54] G. Polesello and D. R. Tovey, *Supersymmetric particle mass measurement with the boost-corrected contransverse mass*, JHEP **1003** (2010) 030, arXiv:0910.0174 [hep-ph].

[55] A. Barr, C. Lester, and P. Stephens, *m(T2) : The Truth behind the glamour*, J. Phys. **G29** (2003) 2343, arXiv:hep-ph/0304226.

[56] T. Melia, *Spin before mass at the LHC*, JHEP **1201** (2012) no. 143, .

[57] ATLAS Collaboration, *Improved luminosity determination in pp collisions at* $\sqrt{s} = 7$ *TeV using the ATLAS detector at the LHC*, arXiv:1302.4393 [hep-ex].

[58] A. L. Read, *Presentation of search results: The CL(s) technique*, J.Phys. **G28** (2002) 2693.

[59] G. Cowan, K. Cranmer, E. Gross, and O. Vitells, *Asymptotic formulae for likelihood-based tests of new physics*, Eur. Phys. J. **C 71** (2011) 1554, arXiv:1007.1727 [physics.data-an].

A Appendix

In Table 8 the number of events selected by the analysis at various stages of the selection is reported for a signal sample with $m(\tilde{t}_1) = 153$ GeV, $m(\tilde{\tau}_1) = 117$ GeV . A total of 150 000 events was generated, which satisfy the condition of having at least two true electron or muon with $p_{\mathrm{T}} > 8$ GeV coming from a decay of a τ. This preselection has an efficiency of 6.4%.

Table 8: Number of simulated events passing various stages of the selection for a signal sample with $m(\tilde{t}_1) = 153$ GeV and $m(\tilde{\tau}_1) = 117$ GeV. Event weights are applied to correct simulated events to data. "Isolation" include the effect of tight ID for electrons and the isolation selection for both electrons and muons. "Cleaning selections" refer to selections applied to remove non-collision backgrounds and detector noise.

Total events	150000
Trigger	10500
Cleaning selections	10000
Two 10 GeV preselected leptons	62800
isolation	52300
opposite sign	52100
$m_{\ell\ell} > 20$ GeV	48400
Leading lepton p_{T}	40600
$\lvert m_{\ell\ell} - m_Z \rvert > 20$ GeV	35400
$\Delta\phi(\mathbf{p}_{\mathrm{T}}^{\mathrm{miss}}, \text{closest jet}) > 1$	26100
$\Delta\phi(\mathbf{p}_{\mathrm{T}}^{\mathrm{miss}}, \mathbf{p}_{\mathrm{Tb}}^{\ell\ell}) < 1.5$	22000
N jets >1	6350
N b-jets > 0	2270
$m_{j\ell} < 180$ GeV	2200
$m_{\mathrm{T2}}^{j\ell} < 70$ GeV	623
$E_{\mathrm{T}}^{\mathrm{miss}}/(E_{\mathrm{T}}^{\mathrm{miss}} + \text{lepton momenta}) > 0.45$	252
$H_{\mathrm{T}}/m_{\mathrm{eff}} < 0.4$	144
$\lvert \Delta x \rvert < 0.04$	138

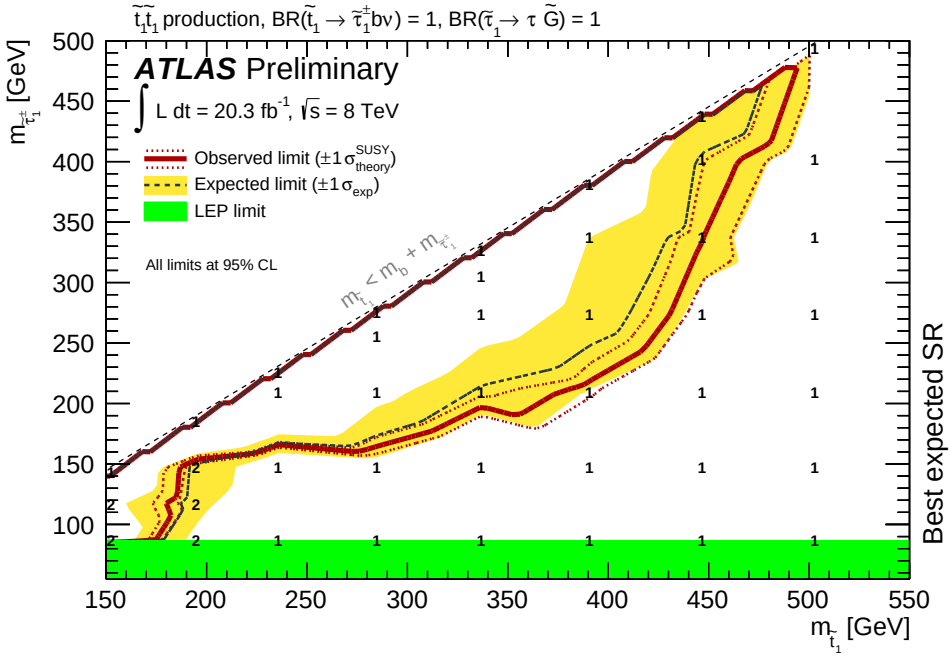

Figure 9: Exclusion limits at 95% CL from the analysis of 20.3 fb^{-1} of 8 TeV collision data on the masses of the top squark and $\tilde{\tau}_1$ and assuming BR($\tilde{t}_1 \to b\tilde{\tau}_1\nu$) = 1. The blue dashed line and the yellow band are the expected limit and its $\pm 1\sigma$ uncertainty, respectively. The thick solid line is the observed limit for the central value of the signal cross section. The dotted lines show the effect on the observed limit when varying the signal cross section by $\pm 1\sigma$ of the theoretical uncertainty. The green band represents the LEP limit [22–26] on the τ slepton mass. The overlaid numbers give the signal region used for the limit calculation: 1 refers to the statistical combination of the signal regions of Ref. [30], while 2 refers to the new signal region.

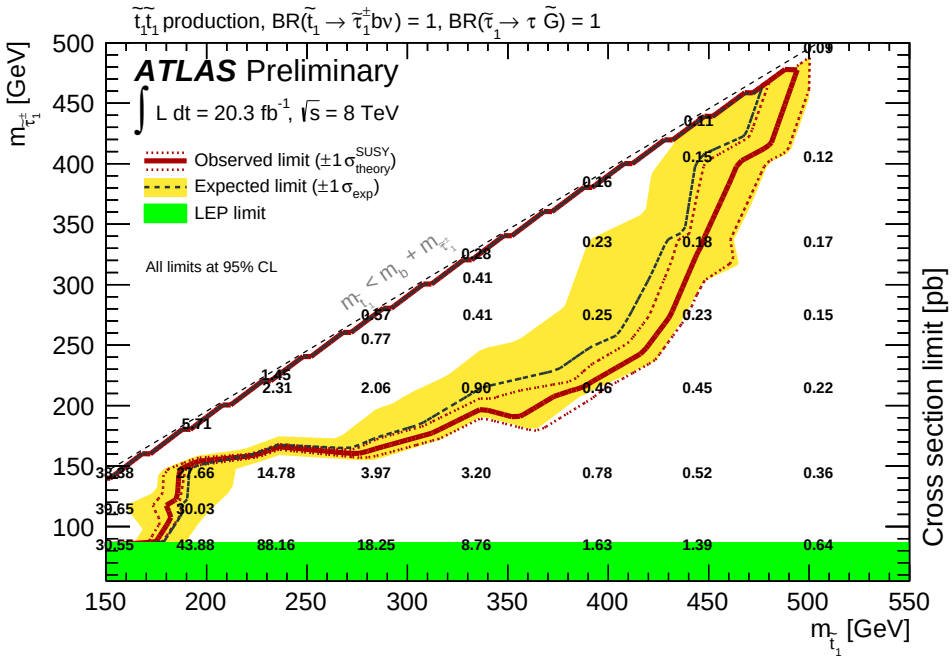

Figure 10: Exclusion limits at 95% CL from the analysis of 20.3 fb^{-1} of 8 TeV collision data on the masses of the top squark and $\tilde{\tau}_1$ and assuming BR($\tilde{t}_1 \to b\tilde{\tau}_1\nu$) = 1. The blue dashed line and the yellow band are the expected limit and its $\pm 1\sigma$ uncertainty, respectively. The thick solid line is the observed limit for the central value of the signal cross section. The dotted lines show the effect on the observed limit when varying the signal cross section by $\pm 1\sigma$ of the theoretical uncertainty. The green band represents the LEP limit [22–26] on the τ slepton mass. The overlaid numbers give the observed upper limit on the signal cross-section for each grid point.